

## **Supplementary Material for**

### **Development of a rapid-shaping and user-friendly membrane**

### **with long-lasting space maintenance for guided bone**

### **regeneration**

#### **Note S1: Fabrication of the GBR membrane.**

PLGA was dissolved in HFIP to achieve a final concentration of 20% (w/v). The resulting solutions were stirred magnetically at room temperature for a duration of 12 hours. Subsequently, the PLGA film was fabricated via electrospinning on an aluminum foil collector, utilizing an electrospinning device for self-assembly. The electrospinning process was conducted under a voltage of approximately 15 kV, employing a 20 G injection needle, and a constant injection rate of 3 mL h<sup>-1</sup>. The distance between the spinneret and collector was maintained at 15 cm. Following electrospinning, the PLGA film was dried in a vacuum oven for a period of 48 hours at a temperature of 25 °C. The film obtained from the aforementioned process was designated as the PLGA film.

The lyophilized GelMA, nanosilicate and I2959 were subjected to sterilization using ethylene oxide, while PEGDA was dissolved in PBS buffer and subsequently filter-sterilized through 0.22 µm filter (produced by Millipore, Burlington, MA, USA). To prepare the PEGDA hydrogel, PEGDA (75% w/v) was dissolved in PBS solution and vigorously stirred using a magnetic stirrer until complete dissolution was achieved (P). Subsequently, GelMA was added to the PEGDA hydrogel at a concentration of 3% w/v (PG). Finally, 4% w/v nanosilicate was then mixed into the PEGDA/GelMA hydrogel to produce PEGDA/GelMA/nanosilicate hydrogel (PGN). Furthermore, GelMA hydrogel and GelMA/nanosilicate hydrogel were prepared using the aforementioned method and ratios for future utilization. Throughout the process, all hydrogels were constantly stirred to ensure uniformity in the system, as depicted in Table S1.

To obtain PLGA film-P, PLGA film-PG, and PLGA film-PGN, each of the three hydrogels (100 µL) was dropped onto an electrospinning PLGA film (10 mm × 10 mm × 0.5 mm). In addition, PLGA film-G and PLGA film-GN were prepared. That is, GelMA and GelMA/nanosilicate hydrogels (100 µL) were dropped onto PLGA film (10 mm × 10 mm × 0.5 mm), respectively. Once the hydrogel soaked the PLGA film completely, the films were then exposed to 365 nm UV light for a period of 30 seconds at room temperature. Following UV treatment, the films were soaked in PBS buffer for 24 hours to achieve complete swelling and removal of any toxic residues. The resulting films were then vacuum dried for later use.

#### **Note S2: Physicochemical characterization**

We employed FTIR (NEXUS 670, United States) to investigate the molecular structure and composition of the prepared materials, namely PLGA film, PLGA film-P, PLGA

film-PG and PLGA film-PGN. The characteristic absorption peaks of functional groups of PLGA, PEGDA, GelMA and nanosilicate were analyzed to provide insight into the molecular composition of the samples. In addition, the elemental composition of PLGA film-PGN was characterized using XPS, which was employed to observe the elemental distribution within the films.

The thermal degradation behavior of the films was characterized using TGA/DSC2, (METTLER TOLEDO, Swiss). The temperature range of 30 to 700 °C was investigated, with a heating rate of 15 °C /min under an inert nitrogen atmosphere. TG analysis was employed to evaluate the effects of the presence of PEGDA and GelMA in the PLGA film-PGN and to assess the incorporation of nanosilicate particles in the film.

The surface wettability of the films was analyzed by measuring the static contact angle of distilled water droplets on the film surface using a standard water contact angle goniometer (Kruss DSC100, Germany). The contact angle was determined by measuring the angle between the line of the horizontal substrate surface and the tangent line of the liquid droplet to the horizontal line at the contacting point. This measurement was conducted five times to ensure accuracy.

The dry weight ( $W_1$ ) of the PLGA film, PLGA film-P, PLGA film-PG, and PLGA film-PGN was obtained by vacuum drying the films for 6 hours at 40 °C. Subsequently, the films were immersed in PBS for 24 h at 37 °C, and the swelling weight ( $W_2$ ) was measured. The degree of swelling was calculated by Eq. (1).<sup>1</sup>

$$\text{Swelling ratio (SR)} = \frac{W_2 - W_1}{W_1} \times 100 \% \quad (1)$$

The PLGA film, PLGA film-P, PLGA film-PG and PLGA film-PGN were subjected to immersion in PBS for 24 h at 37 °C, followed by dehydration in gradient ethanol solutions (30%–100%) and drying. The resulting films were sputter-coated with gold and analyzed using SEM. The elemental composition of the film surface was assessed using energy-dispersive X-ray spectroscopy (EDS, Ultra Plus, Zeiss), including mapping. Furthermore, SEM analysis was also performed on cross sections of PLGA film-P, PLGA film-PG, and PLGA film-PGN. Additionally, the diameter distribution of PLGA electrospun fibers was analyzed using SEM images and ImageJ software (version 1.52k).

To obtain the dry weight ( $W_0$ ) of the PLGA film, PLGA film-P, PLGA film-PG, and PLGA film-PGN, they were vacuum dried for 6 hours at 40 °C. Next, the four films were immersed in 10 mL of PBS solution (pH=7.4) with or without 2 U/mL lysozyme in a shaking incubator at 37°C for 28 weeks. To maintain constant enzyme activity, the lysozyme solutions were replaced with fresh ones every 5 days. At various time intervals, the samples were removed from PBS solution or lysozyme solution, washed twice with sterile deionized water, vacuum dried, and weighted ( $W_t$ ). The degradation rate was calculated by Eq. (2).

$$\text{Degradation Rate (\%)} = \frac{W_0 - W_t}{W_0} \times 100 \% \quad (2)$$

Additionally, after each degradation test in the PBS solution, the pH value of the residual solution in the tube was measured using a pH meter (Leici, China) (n=5). SEM images of PLGA film-PGN were also obtained after being degraded in PBS solution and lysozyme solution for 4 weeks and 28 weeks.

### **Note S3: Tensile mechanical properties**

The mechanical properties of the films were evaluated using a universal testing machine (Instron 5967, United States) at a rate of 0.1 mm/min at 37 °C. Prior to testing, film samples were cut into strips measuring 10 mm in width and 5 cm in length and kept in PBS buffer for 24 hours to allow swelling. Five samples from each group were prepared for wet tensile strength measurements until specimen failure occurred. The elastic modulus, tensile strength, and elongation rate were then calculated from strain-stress curves.

### **Note S4: Cell culture.**

rBMSCs were isolated from the femur and tibia of 10-day-old Sprague-Dawley (SD) rats by flushing out the bone marrow tissue with  $\alpha$ -MEM. The cell suspension was pipetted repeatedly to obtain a homogeneous cell suspension, and after centrifugation to remove blood cells, the remaining adherent cells (rBMSCs) were cultured in a 25 cm<sup>2</sup> cell culture flask in a humid atmosphere at 37 °C with 5% CO<sub>2</sub>. The medium was replaced every two days, and passage-two cells were used for subsequent experiments. To investigate the cellular activities of the films, PLGA film, PLGA film-P, PLGA film-PG, and PLGA film-PGN (each 15 mm in diameter) were fixed on the bottom of 24-well culture plates with glass pressure rings and soaked in the culture medium with 10% FBS overnight. rBMSCs were seeded onto the films at a density of  $1.0 \times 10^5$  cells/mL. After 1 day of cell seeding, three specimens per group were fixed in 4% paraformaldehyde overnight at 4 °C, washed thrice with PBS, and then dehydrated using increasing concentrations of ethanol. The samples were sputter-coated with gold and examined by SEM. To observe the cell adhesion and cell morphology on the films, fluorescent microscopy was also employed. After incubation for 1 or 3 days, the cell was fixed with 4% paraformaldehyde overnight at 4 °C, permeabilized with 0.1% (v/v) Triton X-100 for 30 min at room temperature, then labeled with FITC and DAPI for staining cellular actin filaments and nuclei, respectively. The cells were observed using a fluorescence microscope and their morphological characteristics were analyzed quantitatively.

To prepare the films extracts, 2 mg of each sample (PLGA film, PLGA film-P, PLGA film-PG, and PLGA film-PGN) was immersed in 1 mL of culture medium and incubated for 24 h at 37 °C and 5% CO<sub>2</sub>. Following immersion, the supernatants were collected for subsequent cell culture experiments.

The metabolic functions of rBMSCs and L929 cells were assessed using CCK-8 assay, which measures mitochondrial activity. Cells were seeded on 24-well culture plates at a density of  $5 \times 10^4$  cells per well and incubated with the impregnation solution of the samples for 1, 3, 5, and 7 days. At each time point, non-attached cells were removed by washing the culture plates twice with PBS. Fresh culture medium (1 mL) and CCK-8

solution (100  $\mu$ L) were added to each well, and the plates were incubated at 37  $^{\circ}$ C for 2 h. Subsequently, 80  $\mu$ L of the supernatant was collected in 96-well plates, and the absorbance was determined at a wavelength of 450 nm. Cell viability was calculated by comparing the absorbance values of the experimental and control group. All experiments were performed in triplicate.

To further evaluate the feasibility of the films for GBR, we examined the biocompatibility of the films by measuring cell viability. Cell viability was assessed using a live/dead viability kit ( $n = 5$ ). Briefly, rBMSCs were seeded on four kinds of films and incubated for 1 day, then labeled with 4-IM calcein-AM and 4,5-IM PI for 30 min. After washing with PBS buffer, the films were observed under a fluorescence microscope, and the wavelengths of fluorescence were measured at 490 nm (Calcein-AM, green) and 535 nm (PI, red).

#### **Note S5: Osteogenic differentiation in vitro**

To induce osteogenesis, rBMSCs were cultured at a density of  $1.5 \times 10^5$  cells per well in cell culture medium for 1 day, followed by osteogenic induction medium containing 50  $\mu$ g/mL ascorbic acid, 10 nM dexamethasone, and 5 mM  $\beta$ -glycerophosphate. The medium was refreshed every 2 days. ALP staining was employed to evaluate the ALP activity of rBMSCs after 7 and 14 days of induction. The cells were lysed in 1% Triton X-100 solution at 4  $^{\circ}$ C for 40 min, and the ALP activity and total protein content were measured using the commercially available ALP staining kits and bicinchoninic acid (BCA) protein kits, respectively. The absorbance was measured at 520 nm and 562 nm, respectively, to determine the ALP activity. To assess mineral deposition by rBMSCs, Alizarin Red S staining was performed after osteogenic induction for 14 and 21 days. After rinsing the adherent cells with PBS, the cells were treated with 4% paraformaldehyde, and 1% Alizarin Red solution was applied to stain the adherent cells at 37  $^{\circ}$ C. The calcified nodules were then observed and imaged under a stereomicroscope. To quantify mineralization, the stained nodules were dissolved in 10% cetylpyridinium chloride and the absorbance was measured at 540 nm.

For the real-time polymerase chain reaction (RT-PCR) analysis, we assessed the expression of bone-associated genes, including ALP, runt-related transcription factor 2 (Runx2), and OCN at day 7 and 14. Total RNA extraction was performed using a Universal RNA Extraction Kit (TaKaRa), and RNA concentrations were determined by spectrophotometry. Subsequently, total RNA was reverse-transcribed into complementary DNA (cDNA) using a PrimeScript RT reagent Kit with gDNA Eraser (TaKaRa). RT-PCR for ALP, Runx2, and OCN was conducted using TB Green Premix Ex Taq II (TaKaRa). The relative expression levels of target genes were normalized based on the expression levels of the reference gene  $\beta$ -actin. These reactions were performed in triplicate. Primer sequences (TsingKe) were designed based on established GenBank sequences and are as Table S1:

#### **Table S1**

Primer sequences used for RT-PCR

Name	Primer	Sequence (5' -3' )
$\beta$ -Actin	Forward	CTCTGTGTGGATTGGTGGCT
$\beta$ -Actin	Reverse	CGCAGCTCAGTAACAGTCCG
ALP	Forward	CAACGTGGCCAAGAACATCA
ALP	Reverse	CCTGAGCGTTGGTGTGTAC
Runx2	Forward	CACAAGTGCGGTGCAAACCTT
Runx2	Reverse	AAGAGGCTGTTTGACGCCAT
OCN	Forward	TTATTGTTTGAGGGGCCTGGG
OCN	Reverse	ACACAACCTGCAGGTCGAGTTT

**Note S6: Barrier function of films to fibroblastic cells.**

Each group of films was cut into a 5 mm diameter disk and fixed onto a transwell chamber (Corning). The transwell chamber was placed into a 24-well plate without touching the bottom of the well. L929 cells were suspended in Dulbecco's modified eagle medium (DMEM) supplemented with 10% fetal bovine serum at a density of  $4.0 \times 10^3$  cells/mL. Subsequently, 1 mL of culture medium without cells was added to each well of 24-well plate, and 100  $\mu$ L of the cell suspension was added onto the films in transwell chamber (as shown in Fig. S1C). The transwell chamber was then incubated at 37 °C under a 5% CO<sub>2</sub> atmosphere for 1 day and 3 days. After incubation, the transwell chamber was removed, and the bottom of the 24-well plate was fixed with 4% paraformaldehyde and stained with crystal violet staining solution. The membrane was observed under an inverted phase contrast microscope to determine whether the cells had penetrated through the membrane to the bottom of the well and quantitative analysis.

**Note S7: Biodegradability of films in vivo**

To evaluate biodegradability in vivo, the films were cut into 5  $\times$  5 mm samples, and the dry weight of each sample was recorded as  $W_0$ . The rats were then placed under general anesthesia by injection of 10% chloral hydrate. The films were then subcutaneously implanted into the cranium subcutaneous tissue of the rats, with each animal receiving one film in a subcutaneous pouch. The skin was sutured using non-absorbable 4/0 sutures. At 4 weeks of implantation, the implanted films were excised, and the films were carefully cleaned to remove the adjacent tissue and dried at room temperature. Five parallel samples were used in the experiments. The samples were subsequently vacuum dried and weighed to determine the dry weight of each sample ( $W_t$ ). The degradation rate was calculated using the Eq. (3).

$$\text{Degradation Rate (\%)} = \frac{W_0 - W_t}{W_0} \times 100 \% \quad (3)$$

**Table S2**

Sample	PEGDA % (w/v)	GelMA % (w/v)	Nanosilicate % (w/v)	Abbreviation
PLGA film	-	-	-	PLGA film
PLGA film+ PEGDA hydrogel	75	-	-	PLGA film-P
PLGA film+ PEGDA/GelMA hydrogel	75	3	-	PLGA film-PG
PLGA film+ PEGDA/GelMA/ Nanosilicate hydrogel	75	3	4	PLGA film-PGN

Composition of hydrogels.

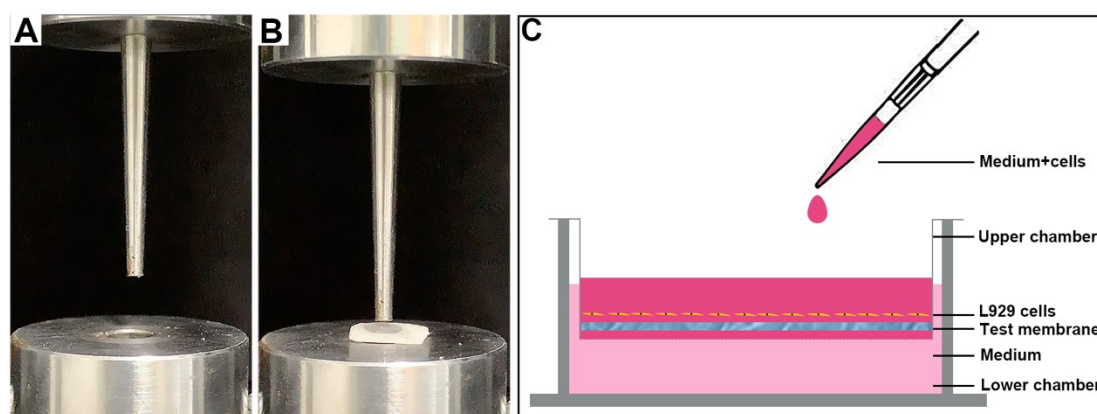


Fig. S1 Schematic illustration. (A) Self-designed upper and lower fixture to test shape maintenance function. (B) Placing calvarial bone slices with films on the lower fixture and aligning the bone defect with the hole of the lower fixture in the experiment. (C) Experimental apparatus for cell barrier performance of the fabricated membranes.

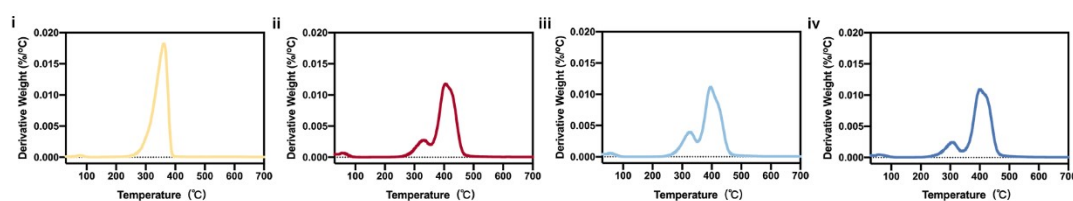


Fig. S2 TG analysis and first derivative to the rate of weight loss. (i. PLGA film; ii. PLGA film-P; iii. PLGA film-PG; iv. PLGA film-PGN)

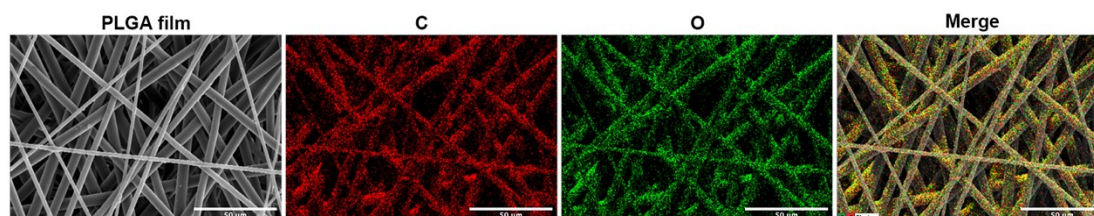


Fig. S3 Energy-dispersive spectroscopy (EDS) element mapping result of PLGA film.

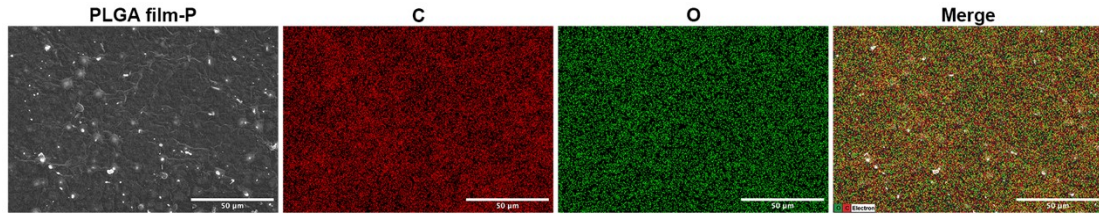


Fig. S4 Energy-dispersive spectroscopy (EDS) element mapping result of PLGA film-P.

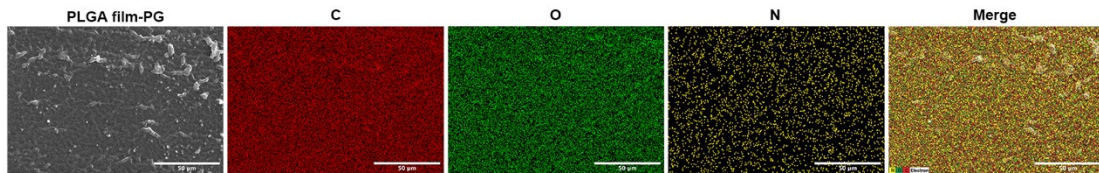


Fig. S5 Energy-dispersive spectroscopy (EDS) element mapping result of PLGA film-PG.

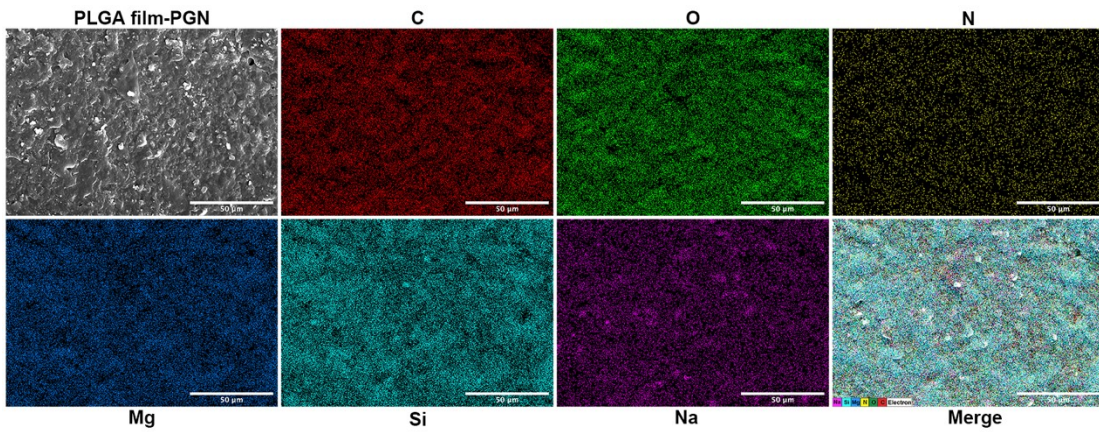


Fig. S6 Energy-dispersive spectroscopy (EDS) element mapping result of PLGA film-PGN.

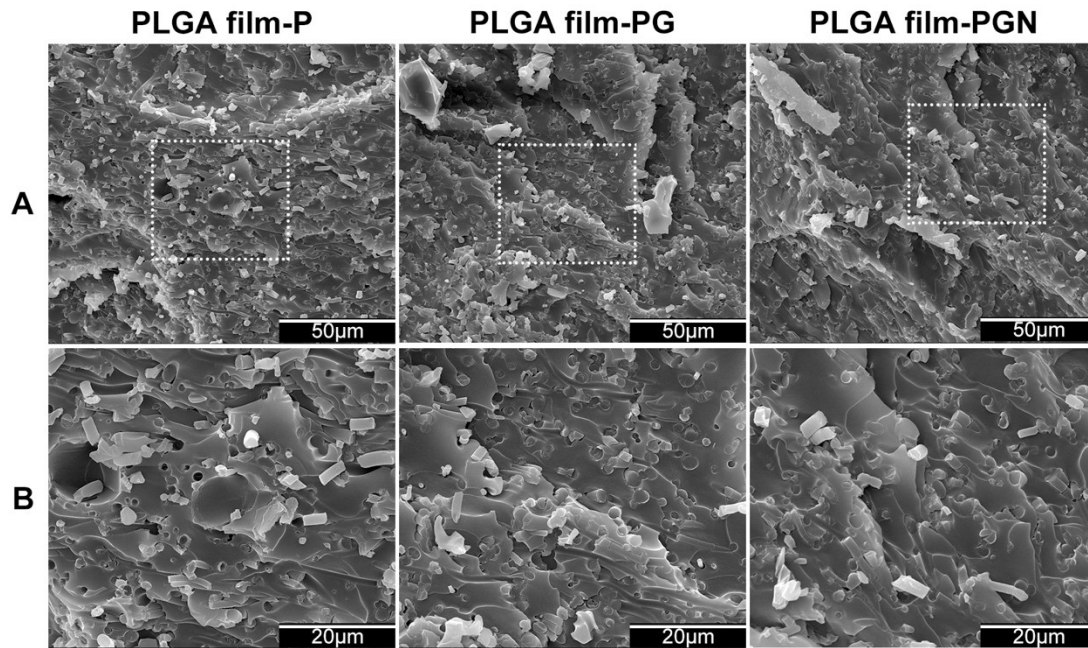


Fig. S7 Cross-sectional SEM image of (A) PLGA film-P, PLGA film-PG, and PLGA film-PGN (scale bar: 50 μm), and (B) white dashed box magnified image (scale bar: 20 μm).

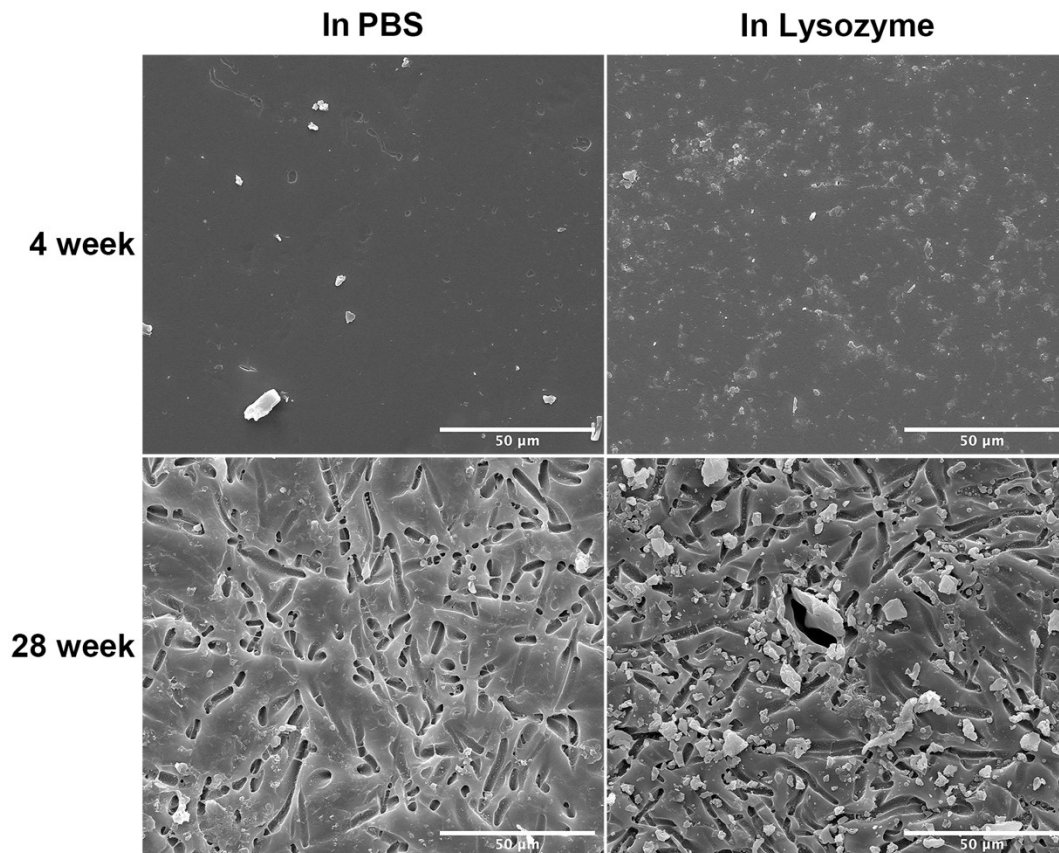


Fig. S8 Scanning electron microscopy (SEM) images of PLGA film-PGN after degraded in PBS solution and lysozyme solution for 4 weeks and 28 weeks.



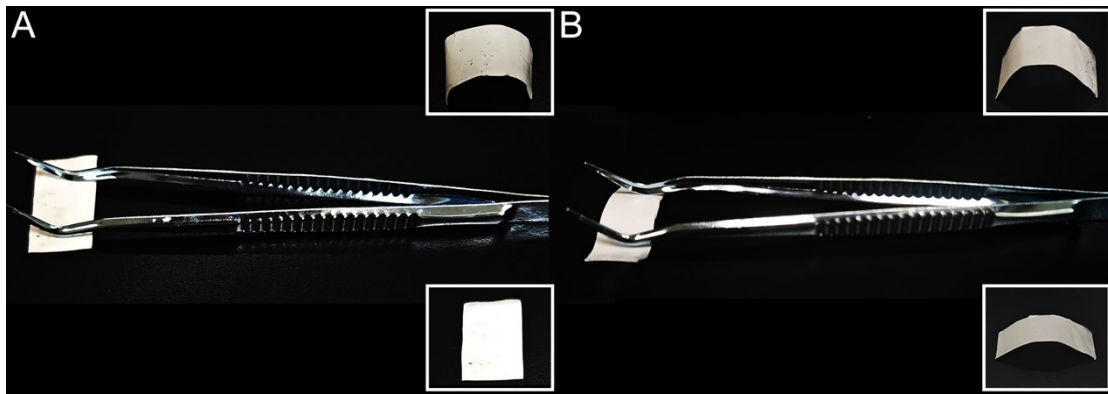


Fig. S9 Plasticity evaluation of PLGA film-G (A) and PLGA film-GN (B) (the image in the upper right is the shape before the force, and the image in the lower right is the shape after the force).

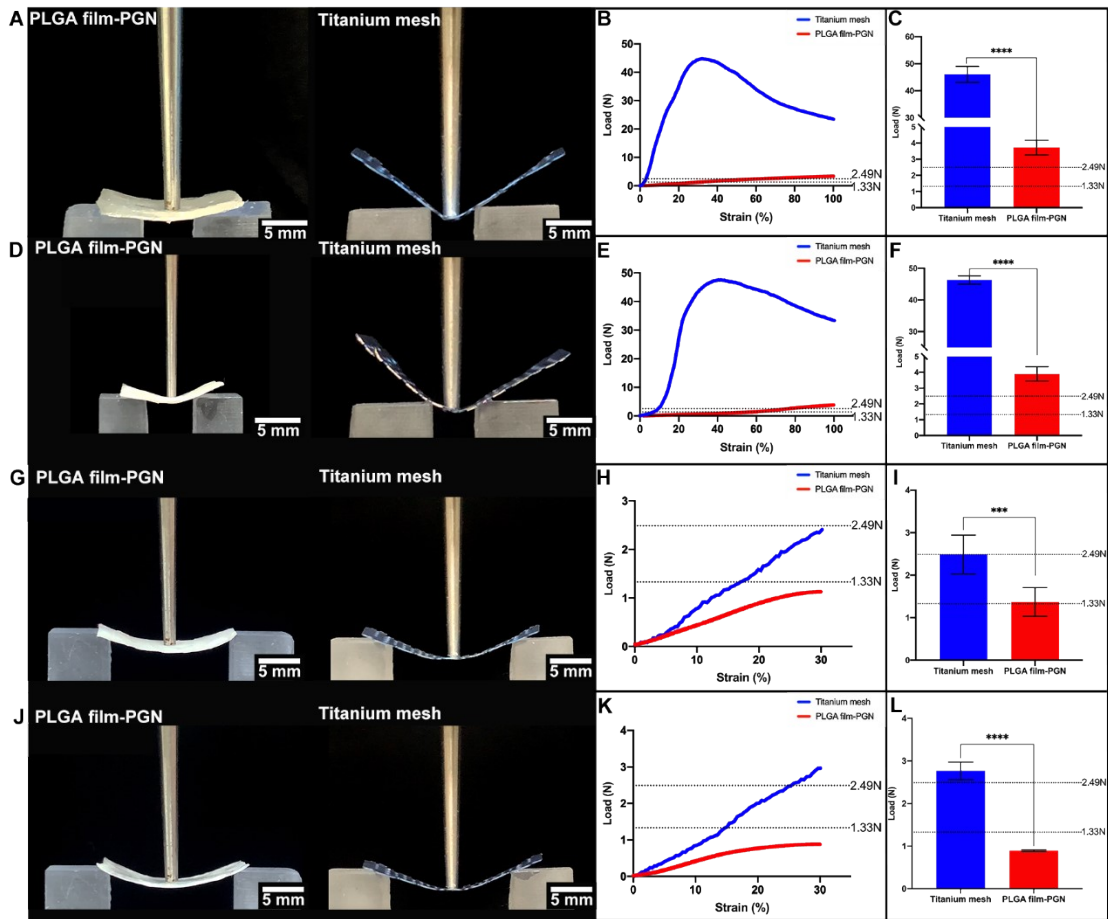


Fig. S10 Bending resistance test. (A) The images of dry PLGA film-PGN and dry titanium mesh during the three-point bending test with a span of 5 mm and a strain of 100 mm. (B) Representative strain-load curves and (C) maximum force (F<sub>max</sub>) of two dry films from three-point bending test with a span of 5 mm. (D) The images of wet PLGA film-PGN and wet titanium mesh during the three-point bending test with a span

of 5 mm and a strain of 100 mm. (E) Representative strain–load curves and (F) maximum force ( $F_{max}$ ) of two wet films from three-point bending test with a span of 5 mm. (G) The images of dry PLGA film-PGN and dry titanium mesh during three-point bending test with a span of 15 mm and a strain of 30 mm. (H) Representative strain–load curves and (I) maximum force ( $F_{max}$ ) of two dry films from three-point bending test with a span of 5 mm. (J) The images of wet PLGA film-PGN and wet titanium mesh during three-point bending test with a span of 15 mm and a strain of 30 mm. (K) Representative strain–load curves and (L) maximum force ( $F_{max}$ ) of two wet films from three-point bending test with a span of 15 mm. ( $n=3$ ,  $*P<0.05$ ,  $**P<0.01$ ,  $***P<0.001$ ,  $****P<0.0001$ )

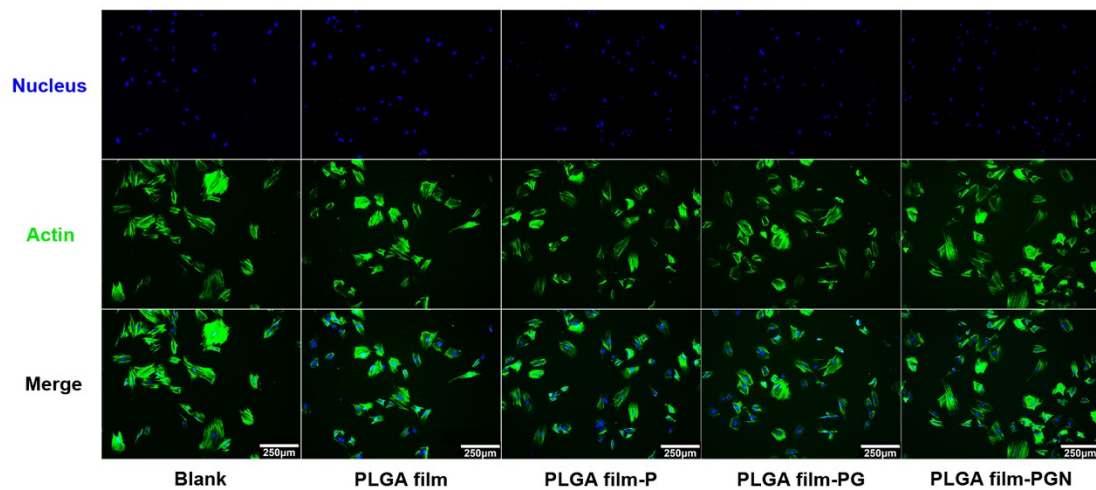


Fig. S11 Cytoskeleton imaging via actin/nucleus staining after a 1-day culture of rBMSC cells.

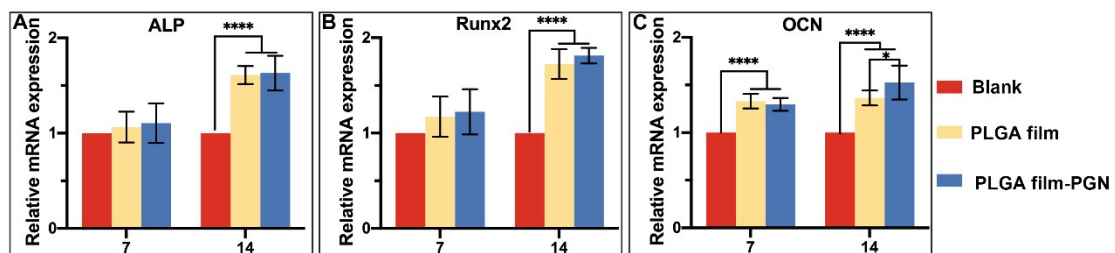


Fig. S12 Real-time PCR analysis of the mRNA expression of ALP, Runx2, and OCN. ( $n=3$ ,  $*P<0.05$ ,  $**P<0.01$ ,  $***P<0.001$ ,  $****P<0.0001$ )

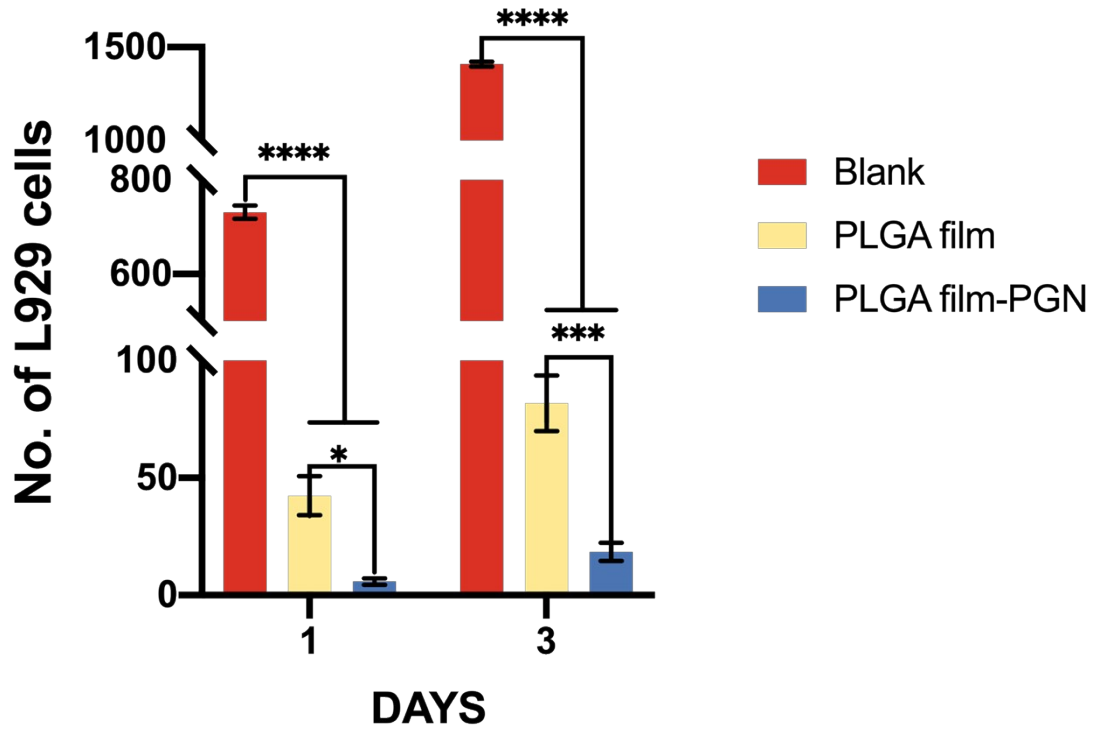


Fig. S13 Quantitative analysis of the barrier function.

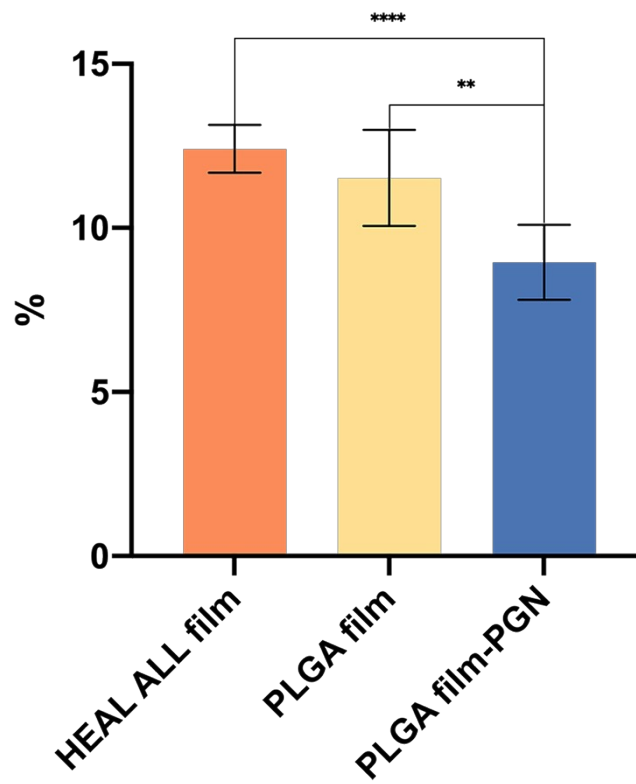


Fig. S14 Mass loss over 4-weeks degradation in vivo of the three films. (n=3, \*P<0.05,

\*\*P<0.01, \*\*\*P<0.001, \*\*\*\*P<0.0001)

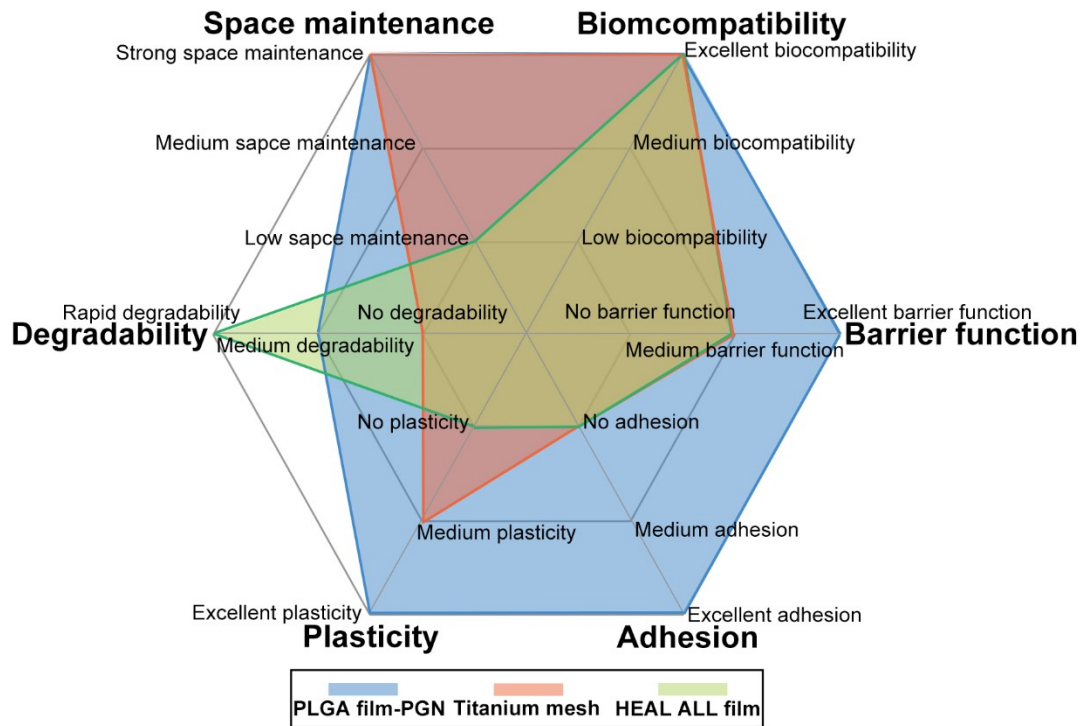


Fig. S15 Application comparison. Comparison of the performance of PLGA film-PGN with some commercially available GBR membrane.

## References

- 1 X. Zheng, X. Zhang, Y. Wang, Y. Liu, Y. Pan, Y. Li, M. Ji, X. Zhao, S. Huang, *Bioact. Mater.*, 2021, 6, 3485–3495.